

# Role of hepcidin and its downstream proteins in early brain injury after experimental subarachnoid hemorrhage in rats

Guanping Tan<sup>1</sup> · Liu Liu<sup>1</sup> · Zhaohui He<sup>1</sup> · Jiujuan Sun<sup>1</sup> · Wenli Xing<sup>1</sup> · Xiaochuan Sun<sup>1</sup>

Received: 6 January 2016 / Accepted: 25 March 2016 / Published online: 1 June 2016  
© Springer Science+Business Media New York 2016

**Abstract** Early brain injury (EBI) is a major cause of mortality from subarachnoid hemorrhage (SAH). We aimed to study the pathophysiology of EBI and explore the role of hepcidin, a protein involved in iron homeostatic regulation, and its downstream proteins. One hundred and thirty-two male Sprague–Dawley rats were assigned into groups ( $n = 24/\text{group}$ ): sham, SAH, SAH + hepcidin, SAH + hepcidin-targeting small interfering ribonucleic acid (siRNA), and SAH + scramble siRNA. Three hepcidin-targeting siRNAs and one scramble siRNA for hepcidin were injected 24 h before hemorrhage induction, and hepcidin protein was injected 30 min before induction. The rats were neurologically evaluated at 24 h and euthanized at 72 h. Hepcidin, ferroportin-1, and ceruloplasmin protein expression were measured by immunohistochemistry and Western blotting. Brain water content, blood–brain barrier (BBB) leakage, non-heme tissue iron and Garcia scale were evaluated. Hepcidin expression increased in the cerebral cortex and hippocampus after experimental SAH ( $P < 0.05$  compared to sham), while ferroportin-1 and ceruloplasmin decreased ( $P < 0.05$ ). Hepcidin injection lowered the expression of ferroportin-1 and ceruloplasmin further but siRNA reduced the levels of hepcidin ( $P < 0.05$  compared to SAH) resulting in recovery of ferroportin-1 and ceruloplasmin levels. Apoptosis was increased in SAH rats compared to sham ( $P < 0.05$ ) and increased slightly more by hepcidin, but decreased by siRNA ( $P < 0.05$  compared to SAH). SAH rats had lower neurological scores, high brain water content, BBB permeability, and non-heme

tissue iron ( $P < 0.05$ ). In conclusion, downregulation of ferroportin-1 and ceruloplasmin caused by hepcidin enhanced iron-dependent oxidative damage and may be the potential mechanism of SAH.

**Keywords** Early brain injury · Subarachnoid hemorrhage · Hepcidin · siRNA · Apoptosis · Rats

## Introduction

Early brain injury (EBI) has become an important direction for study of subarachnoid hemorrhage (SAH). A number of key factors are associated with EBI including elevation of intracranial pressure, reduction of cerebral blood flow, suppression of cerebral perfusion pressure, fall in brain oxygenation, blood–brain barrier (BBB) breakdown, brain edema, and neuronal cell death [1]. EBI is the leading cause of mortality in patients with SAH, resulting in it becoming the primary direction of SAH research [2]. Matz et al. [3] firstly demonstrated the involvement of apoptosis in early brain injury following SAH. Our prospective studies have conclusively demonstrated that extensive protein damage after SAH leads to overloading endoplasmic reticulum (ER) with aberrant and unfolded proteins, and ER stress activates apoptosis [4].

The involvement of the CCAAT/enhancer binding protein (C/EBP) homologous protein (CHOP alias DDIT3/GADD153) in ER stress has been found to be a major inducer of apoptosis after SAH, and CHOP silencing leads to reduction of apoptosis and other injury after SAH [4]. There is a C/EBP-binding site on the hepcidin gene. C/EBP $\alpha$  inhibits the expression of other members of C/EBP family, and CHOP exhausts this inhibition and enhances the expression of hepcidin [5, 6]; we suspect that

✉ Zhaohui He  
geno\_he@163.com

<sup>1</sup> Department of Neurosurgery, First Affiliated Hospital of Chongqing Medical University, Chongqing 400042, China

the up-regulated expression of hepcidin exacerbates apoptosis. Hepcidin regulates cellular iron efflux by inducing internalization of ferroportin-1 (Fpn1) [7]. Li et al. [8] have also found that hepcidin modulates the expression of ceruloplasmin (CP) and Fpn1 in rat cerebral cortex and hippocampus.

Hepcidin is a polypeptide secreted by the liver. Pigeon et al. [9] have reported hepcidin's role in iron homeostatic regulation. Hepcidin can also regulate the expression of Fpn1 and decrease the transfer rate of iron by directly acting on the epithelial cells of small intestine [10]. Nemeth has found that Fpn1 is the receptor for hepcidin, and it can downregulate the expression of Fpn1 and increase Fpn1 degradation. All these effects can cause the accumulation of iron in the cell, which is considered to be one of the key factors of apoptosis.

CP is a ferrous oxidase, which can promote a ferrous iron to oxidize to ferric iron. Only the ferric iron can unite with transferrin. CP plays an important role in iron-transport systems and iron steady state. CP is unable to pass BBB [11]. Klomp [12] has reported the expression of CP in the central nervous system of both humans and rats, especially in the cerebral cortex, basal ganglia cells, hippocampus, cerebellum, and corpus callosum. This suggests that CP can be synthesized and secreted by brain tissues.

In this study, it was postulated that the overexpression of hepcidin could lead to abnormal iron deposition in neurons, which in turn could play a key role in the pathological process of EBI after SAH.

## Materials and methods

### Animals and groups

One hundred and thirty-two male Sprague–Dawley rats (Chongqing Medical University, Chongqing, China) weighing 280–350 g were used in this study. The animal experimental ethics committee of Chongqing Medical University approved the experimental protocol. All the rats were randomly assigned to the following groups ( $n = 24$  in each group): sham, SAH, SAH + hepcidin, SAH + hepcidin-targeting small interfering ribonucleic acid (siRNA), and SAH + scramble siRNA. Three hepcidin-targeting siRNAs and one scramble siRNA for hepcidin were injected 24 h before hemorrhage induction, and hepcidin protein were injected 30 min before hemorrhage induction. The rats were anesthetized with 3.5 % chloral hydrate (10 ml/kg intraperitoneally) and perfused with phosphate buffer solution (PBS) at 24 h following SAH; the brain was collected for molecular biological analysis, followed by administration of 10 % buffered formalin for immunohistochemistry. To determine the brain water content and

neurobehavioral tests, brain was collected at 72 h after SAH.

### Experimental SAH model

The experimental SAH model was produced using stereotaxic insertion of a catheter with a rounded tip and a side hole into the prechiasmatic cistern as reported by Wang et al. [13]. We made small improvements. A tiny and soft plastic tube was used. Anesthesia was performed during the SAH induction with 3.5 % chloral hydrate (10 ml/kg intraperitoneal injection). The experimental SAH model was made by drilling a small hole (with a dentist' micro-drill; 7.5 mm anterior to bregma in the midline) in the skull and injecting non-heparinized fresh autologous arterial blood. The tube was leaned forward 45° in the sagittal plane and lowered until it reached the base of the skull. It was retracted 0.5 mm in order to inject the arterial blood satisfactorily. To prevent the cerebrospinal fluid and blood coming out of the hole, the burr hole was plugged with bone wax before inserting the tube. About 0.3 ml arterial blood was slowly injected into the prechiasmatic cistern for 20 s with a syringe pump under aseptic technique. Control groups were injected with 0.3 ml saline. The awaking time of anesthesia was about 30 min. The rats were returned to cages after anesthesia resuscitation, and the room temperature was kept at  $23 \pm 1$  °C. To prevent dehydration, 20 ml of 0.9 % saline was injected subcutaneously right after the operation. The average mortality of SAH was 9.09 %, and no mortality was recorded in the sham-operated rats.

### siRNA injection

Animals were anesthetized with 3.5 % chloral hydrate (10 ml/kg intraperitoneally). They were positioned in a stereotactic device; a small hole (1 mm) was drilled through the skull with a dentist's micro-drill, and a 5- $\mu$ l microsyringe was inserted stereotaxically into the right lateral ventricle (coordinates: 0.6 mm posterior, 4.5 mm ventral, and 1.6 mm lateral to the bregma) [14]. Three hepcidin-targeting siRNAs and one scramble siRNA (20  $\mu$ M stock solution; GENECHM, Shanghai, China) were injected at a rate of 1  $\mu$ l/min with the 5  $\mu$ l microsyringe. The sequence of the first siRNA for hepcidin was sense, 5'GUCUCUGUUGCAUAACAUA; antisense, 5'UAUGUUAUGCAACAGAGAC. The second siRNA sequence was sense, 5'UGCCUCUUCUGCUGUAAAU; antisense, 5'AUUUACAGCAGAAGAGGCA. The third siRNA sequence was sense, 5'UGCUGUAAGAAUUCUCCU; antisense, 5'AGGAGGAAUUCUUACAGCA. Scrambled RNA served as a control. The syringe was

removed after the injection; the skull hole was filled with bone wax, and the skin incision was stitched closed.

### Brain water content

Brains were removed at 72 h after SAH, and the hemispheres were separated and weighed to assess their wet weight (WW). The hemispheres were then dried for 24 h at 100 °C in the oven and their dry weight (DW) was determined. Brain water content (%) was calculated using the following formula:  $[(WW - DW)/WW] \times 100$  [15].

### Evans blue dye extravasation

Disruption of BBB was analyzed 24 h after the SAH using Evans blue (EB), as reported previously [16]. Rats were anesthetized, and EB dye (4 %; 2.5 ml/kg) was injected into the caudal vein and allowed to circulate for 1 h. Rats were perfused with PBS. The amount of extravasated EB in the brain was determined by spectrofluorometry at excitation wavelength 610 nm, emission wavelength of 680 nm, and bandwidth of 10 nm.

### Nonheme brain tissue iron determination

Rats were anesthetized and killed at 72 h after SAH. The brains were perfused with 0.1 mol/l cold saline before decapitation. The remaining subarachnoid blood was carefully removed from the basal surface of the brain. Hippocampal tissues were separated, weighed and homogenized. 1 ml of 8.5 mol/l HCl was added to the samples. Hippocampal tissues were hydrolyzed at 90 °C for 1 h. Tissues were treated with 2 ml of 20 % trichloroacetic acid (TCA) to precipitate the proteins after cooling. After centrifugation the supernatant was collected. The precipitate was washed with 1 ml of 4.25 mol/l HCl plus 20 % TCA (1:1). 4 ml of 1 mol/l sodium citrate was added to the supernatant and the pH was adjusted to 3.1. We used a spectrophotometer to determine the nonheme iron concentration and ferrozine as color reagent.

### Garcia behavioral assessment

The neurological deficits of the rats were examined by the Garcia behavioral assessment 24 h after SAH as previously described [17]. This involved evaluation of the rats and scoring them based on various parameters, which included spontaneous activity, circling behavior, symmetry of movement and outstretch of limbs, body proprioception, climbing ability, and vibrissae touch. The scale was scored from 3 to 18.

### Immunohistochemistry

Immunohistochemistry was used to detect the expression of hepcidin and its downstream proteins, Fpn1 and CP, as described [18]. Animals were transcardially perfused under anesthesia with 3.5 % chloral hydrate and PBS followed by 4 % paraformaldehyde at 24 h after SAH. Brains were fixed for 48 h, placed in 30 % sucrose in PBS, embedded by paraffin, and were then used to make routine paraffin sections. To quench the endogenous peroxidase activity, we washed the sections with 0.01 mol/l PBS and incubated them in 0.6 % H<sub>2</sub>O<sub>2</sub> for 20 min. Antigen retrieval was performed in a microwave oven at 100 °C for 15 min in citrate buffer, pH 6.0. The sections were blocked with goat serum in PBS for 1 h, and then incubated overnight at 4 °C, respectively, with rabbit anti-hepcidin, Fpn1 and CP polyclonal antibodies (1:500; all purchased from Abcam, Cambridge, MA, USA). After washing three times with PBS for 10 min, the sections were incubated at 37 °C for 15 min with biotinylated goat anti-rabbit secondary antibody (1:250; ZSGB-BIO, Beijing, China). The sections were washed three times for 10 min and incubated with streptavidin-horseradish peroxidase conjugate (1:250; ZSGB-BIO) for 15 min at 37 °C. After being washed three times for 10 min diaminobenzidine tetrahydrochloride (DAB) was used as the chromogen. The sections were stained with hematoxylin, dehydrated in ethanol, covered with neutral balsam. Finally, the sections were photographed with an Olympus (BX51, Japan) microscope with a DP controller set to the same parameters for each section (sensitivity: ISO 200; exposure time: 1/4.0 s; spot: 30 %; accumulation mode: average; objective: 910; and field diaphragm: 0.75). The same areas were selected in the cortex (pyramidal layer cells of ectorhinal cortex) and in the hippocampus (cells in the hippocampus CA1 area and granular layers in dentate gyrus) between control and experimental groups to take photographs. All the photographs were analyzed with professional software (Image-Pro plus 6.0), and the area of interest was set as the whole image. The intensity was calibrated with standard optical density (OD). The background gray level was set (manual color select, count/size column) at 150 in all slices of control and experimental groups, and counts of 150–225 (max) signals were noted in the histogram. To filter the non-cellular structure signal in the background, the range of area was set as 2000 pixels. The positive area was then counted to get the mean density (MD).

### Quantitative cell count

The levels of apoptotic cells were measured by quantitative cells count. Xylene deparaffinized sections were hydrated by subsequent incubation in 100 and 95 % ethanol,

respectively. Then, samples were incubated with 0.2 % Triton X-100 in PBS-Tween for 30 min. Endogenous peroxidase was blocked by incubation in 3 % H<sub>2</sub>O<sub>2</sub> in PBS for 10 min. Then, the sections were pre-incubated in Terminal Transferase (TdT) Reaction Buffer (Roche Diagnostic, USA) for 10 min followed by treatment with TdT Reaction Mixture (Roche Diagnostic) for 1 h at 37 °C. For detection, sections were incubated with Streptavidin-HRP in PBS for 20 min at room temperature, followed by treatment with 3, 3'-diaminobenzidine (DAB) for 1–2 min. Counterstaining was carried out with hematoxylin for 30 s. The sections were finally dehydrated by ethanol gradient before mounting. TUNEL-positive cells were counted in a blinded manner. A specific area in the cerebral cortex was averaged from six photomicrographs from each animal. Six rats per group were used for quantitative histology analysis.

### Western blot analysis

Cerebral cortex and hippocampus were ground and homogenized in the radioimmunoprecipitation assay buffer containing protease/phosphatase inhibitors. The supernatant was collected after centrifugation at 12,000g for 15 min at 4 °C. The aliquots of 20 µg of total protein were run on 10 % sodium dodecyl sulfate polyacrylamide gel electrophoresis (Beyotime, Wuhan, China) and transferred onto polyvinylidene fluoride membranes. The membranes were blocked in 5 % non-fat milk containing Tris-buffered saline and Tween 20 (20 mmol/l Tris-hydrochloride, pH 7.6, 137 mmol/l sodium chloride, 0.1 % Tween-20) for 2 h at room temperature and probed at 4 °C overnight with the following primary antibodies (Abcam; all diluted 1:300, SLC40A1 diluted 1:1000): anti-hepcidin-25 antibody (ab81010), anti-ceruloplasmin antibody (ab110449), anti-SLC40A1 antibody (ab85370), and glyceraldehyde 3-phosphate dehydrogenase (GAPDH). They were then incubated for 2 h at room temperature with respective secondary antibodies (horseradish peroxidase-labeled antibody, Beyotime) diluted 1:2000. Electrochemiluminescence substrate kit reagents (Millipore, Billerica, MA, USA) were used to detect the target protein using exposure of Kodak (6535876) radiographic films. The proteins were quantified by Quantity One software. The results were expressed relative to GAPDH bands from the same blot and normalized with regard to sham [4].

### Statistical analysis

Data are expressed as mean ± SEM. Statistical significance was determined by analysis of variance, followed by *T* test for multiple comparisons. A probability value of *P* < 0.05 was taken to be statistically significant. All the results were analyzed by SPSS 18.0 software.

## Results

### Brain damage was attenuated with hepcidin siRNA treatment

The SAH model had induced brain injury in the rats. At 72 h after SAH, the brain water content increased by 2.27 % in the SAH group (78.00 %, sham 75.73 %). The EB contents of the brain tissue described the disruption of BBB 24 h after SAH (*n* = 6 for each group) for the SAH group this was 0.450 ± 0.010 ng/mg compared to 0.404 ± 0.010 ng/mg for the sham group (*P* < 0.05). SAH also increased the nonheme iron levels and decreased the Carcia scale compared to the sham group (*P* < 0.05, Fig. 1).

Hepcidin injection increased the brain water content further (81.07 %), but this was decreased significantly towards the sham levels by hepcidin-targeting siRNA treatment (76.81 %, *P* < 0.05 compared to SAH group), as shown in Fig. 1a.

Hepcidin-injection also increased EB content to 0.484 ± 0.018, but this was reduced by hepcidin-targeting siRNA treatment towards sham levels at 0.428 ± 0.004 (*P* < 0.05 compared to SAH and hepcidin injection groups), but not in the scramble siRNA injection groups at 0.448 ± 0.010 ng/mg (Fig. 1b).

Nonheme iron levels increased further in the hepcidin injection group (122.26 ± 7.86) (Fig. 1c). But the increase in nonheme iron levels was markedly reduced by hepcidin-targeting siRNA treatment (76.51 ± 6.29, *P* < 0.05 compared to both SAH and hepcidin injection group).

### Expression of hepcidin, Fpn1, and CP was regulated after SAH modeling

Hepcidin was distributed in different brain regions including the olfactory bulb, cortex, hippocampus, and amygdala. There was a marked increase of hepcidin expression in SAH model rats compared with the sham group (0.0043 in sham, 0.0205 in SAH, mean density, *P* < 0.05). Downstream target protein levels were also decreased in the SAH rats (Fpn1, sham 0.0045, compared with SAH 0.0145; CP sham 0.0015, compared with SAH 0.0116; *P* < 0.05) (Fig. 2). The regulation of hepcidin on Fpn1 and CP was more obvious in the cerebral cortex than other regions.

### Hepc-targeting siRNA treatment significantly decreased the number of apoptotic cells after SAH

The quantitative analysis of cells with apoptotic labeling (TUNEL) in the cerebral cortex is demonstrated in Fig. 3.



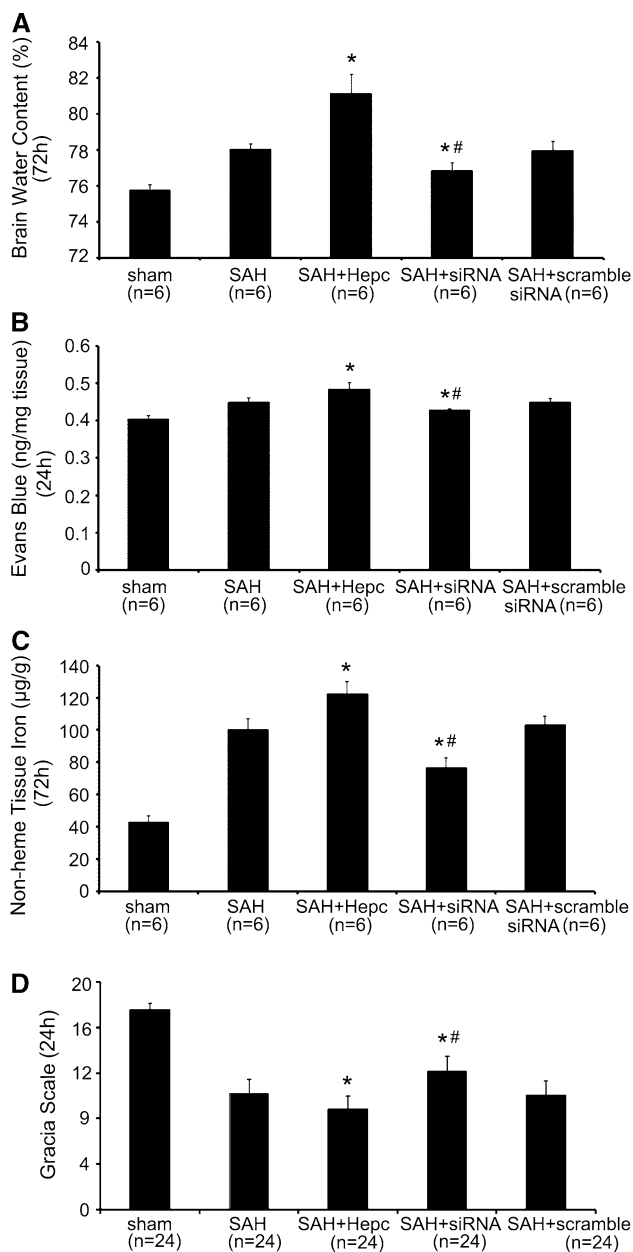


**Fig. 1** Brain water content, blood brain barrier (BBB) leakage, non-heme tissue iron and neurological scores of each group of rats. **a** brain water content, **b** Evans blue extravasation, **c** non-heme iron concentration in the hippocampal tissues at 72 h post-subarachnoid hemorrhage (SAH). **d** Garcia scale of rats in each group at 24 h post SAH. *Hepc* hepcidin. \* $P < 0.05$  versus SAH group. # $P < 0.05$  versus SAH + Hepc group

In the cerebral cortex, the number of TUNEL-positive cells was 35 for hepcidin-targeting siRNA compared with 64 for the SAH group ( $P < 0.05$ ). The number of TUNEL-positive cells after hepcidin injection was significantly higher than the SAH group (87,  $P < 0.05$ ), while there was almost no TUNEL-positive cells in the sham group.

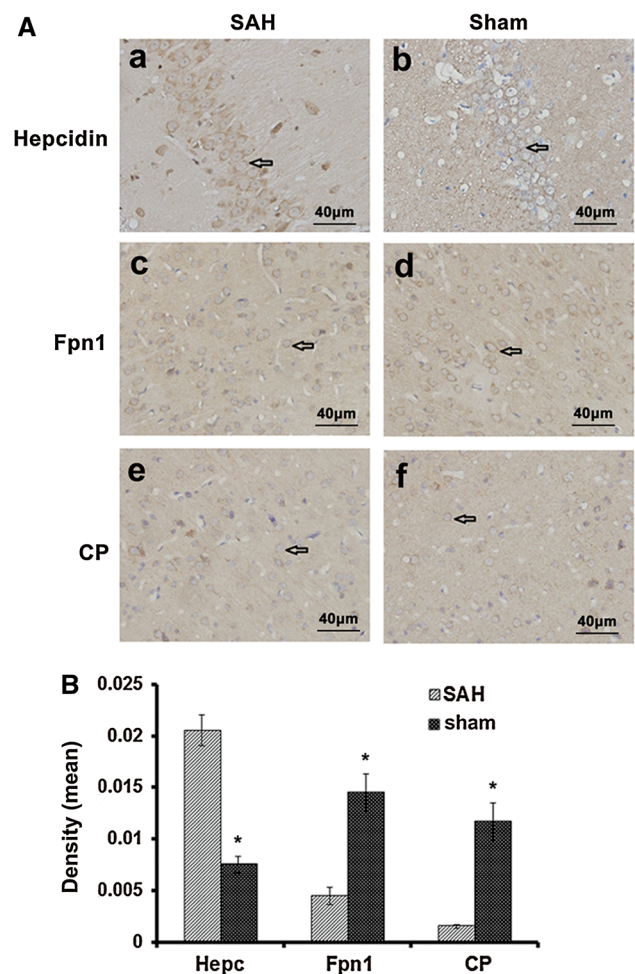
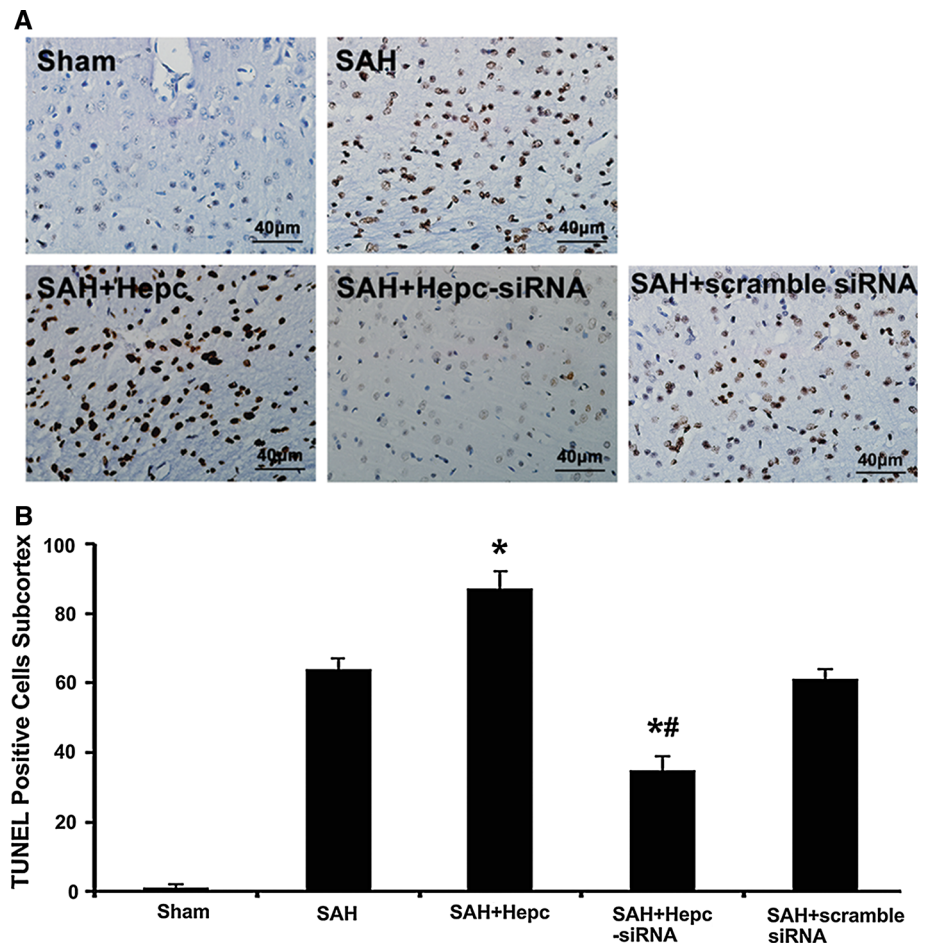


**Fig. 2** Immunohistochemistry of hepcidin, ferroportin-1 (Fpn1), and ceruloplasmin (CP) expression in the hippocampus and cortex of subarachnoid hemorrhage (SAH) rats. **a** example images from the SAH rats compared to the sham rats. Hepcidin, Fpn1, and CP positive staining were observed on and among cell bodies. **b** The mean density of the positive staining was measured by Image Pro Plus 6.0 software. Data are presented as mean  $\pm$  SEM, versus control, \* $P < 0.05$  versus SAH group

### Expression of hepcidin, Fpn1, and CP was reversed after hepcidin siRNA treatment

The higher levels of hepcidin expression in cerebral tissue (SAH 1.98-fold, sham 0.51-fold,  $P < 0.05$ ), and decreased expression of its downstream targets (SAH Fpn1 0.43-fold, CP 0.70-fold; sham Fpn1 0.60-fold, CP 1.08-fold;  $P < 0.05$ ) were investigated in more detail. Hepcidin-targeting siRNA injection reduced the hepcidin protein level (0.73-fold), which caused overexpression of CP and Fpn1 (0.48-fold and 0.77-fold). Therefore, hepcidin-targeting siRNA injection prevented hepcidin-induced Fpn1 and CP down-regulation. Scramble siRNA treatment showed increased expression of hepcidin, but the treatment failed

**Fig. 3** Apoptosis in the cerebral cortex of the rat groups. **a** Images of TUNEL-positive cells in the brain. **b** Graphs show numbers of apoptotic cells in the cerebral cortex. *Hepc* hepcidin, *SAH* subarachnoid hemorrhage. \* $P < 0.05$  versus SAH group. # $P < 0.05$  versus SAH + *Hepc* group



to reduce the level of downstream protein (Hepcidin 1.14-fold; *Fpn1* 0.40-fold, *CP* 0.54-fold,  $P < 0.05$ ). Scramble siRNA injection had no influence on the expression of hepcidin and downstream proteins (Fig. 4).

## Discussion

The purpose of this study was to investigate the pathophysiology of EBI and the role hepcidin might play in the process. We found that SAH rats showed higher levels of hepcidin with lower expression levels of its downstream targets *Fpn1* and *CP*. The SAH rats developed EBI and this was increased by injection of hepcidin but decreased by hepcidin-targeting siRNA. Apoptosis was evident in the cerebral cortex of SAH rats and hepcidin injection significantly increased this level, but hepcidin-targeting siRNA decreased it. These results suggest that hepcidin plays a key role in the pathological process of EBI after SAH and might assist with the development of novel treatment strategies.

In this study, we found that SAH induces an increase of brain water content (2.27 %, compared to sham),

aggravates blood–brain barrier leakage (12.5 %, compared to sham), and increases the nonheme iron concentration in hippocampal tissues (134.5 %, compared to sham). This effect can be mediated by iron metabolism disorder. It is generally agreed that hemoglobin degradation products including iron can cause increased intracellular iron levels [19]. But new results suggest that iron metabolism disorder could also increase the iron content of cells [20]. This could also increase neuronal apoptosis in the hippocampal gyrus CA1 area. In patients with aceruloplasminemia [21], the accumulation of iron can be found in many tissues and organs including those of the central nervous system. This indicates the role of *CP* in iron metabolic regulation. Reactive oxygen species (ROS) are produced during the course of organism supersession, which can be enhanced by iron. The enhanced reactivity of ROS produces hydroxyl radicals and aggravates oxidative damage of biomolecules. Iron-induced calcium metabolism disorder is an important additional contributor to apoptosis [22–24]. It has confirmed that ROS can induce apoptosis by many mechanisms in models of brain injury, including the mitochondrial pathway that plays an important role, e.g., cytosolic cytochrome *c* release and subsequent caspase

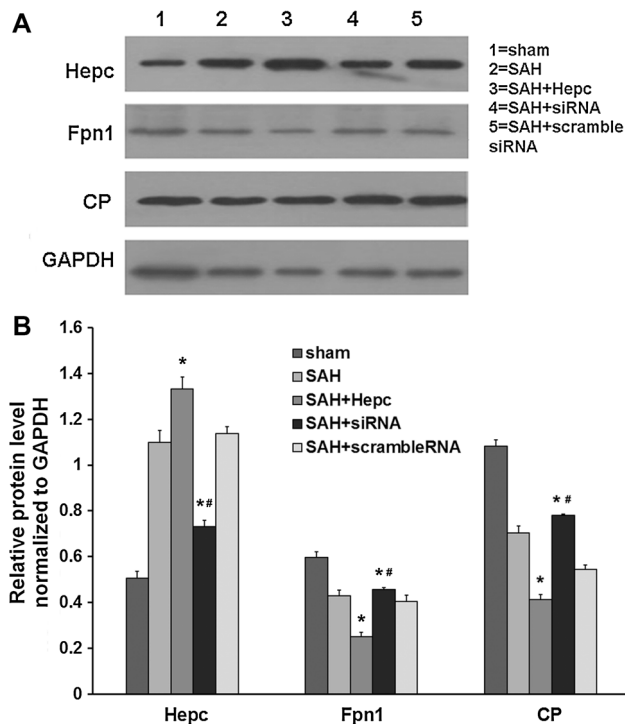


**Fig. 4** Expression of hepcidin, ferroportin-1 (Fpn1), and ceruloplasmin (CP) in each group. **a** Western blot images of the protein expression levels in the cerebral cortex and hippocampus. **b** Quantitative analysis of the protein expression levels. All protein levels were compared to the housekeeping gene GAPDH levels from the same blot to ensure consistent loading of the protein on the gel. *Hepc* hepcidin, *SAH* subarachnoid hemorrhage. \* $P < 0.05$  versus SAH group. # $P < 0.05$  versus SAH + Hepc group

activation [25–28]. The results of this study also indicated that hepcidin-targeting siRNA treatment mitigates the brain damage in the rat model of SAH. Inhibition of Fpn1 and CP levels by hepcidin after SAH was counteracted by hepcidin-targeting siRNA injection. The increased expression of Fpn1 and CP was likely to have enhanced the transportation of diatomic iron and also improved diatomic iron accumulation. Therefore, reduced apoptosis was seen with hepcidin-targeting siRNA treatment. Our results indicated that SAH could induce apoptosis of hippocampal pyramidal cells and cortical neurons probably by activating ER stress. The overexpression of CHOP in ER stress was previously found to be the other major contributor. Inhibition of CHOP expression can significantly reduce the apoptosis of neurons, decrease BBB permeability and brain water content, improve neurological [4], and also attenuate cerebral vasospasm [29].

The results of the present study, therefore, suggest a link between ER stress and iron metabolism. Hepcidin was upregulated after SAH, and the expression of downstream targets like Fpn1 and CP was inhibited. All of these effects

led to excessive iron accumulation and promoted apoptosis. Apoptosis can aggravate the destruction of BBB, increase the brain water content, and decrease the neurological scores. The treatments of hepcidin-targeting siRNA to inhibit the expression of hepcidin and promote the expression of downstream proteins and improved the results of functional assessment.

This study has some limitations; these include the use of a classic method of determining the brain water content by wet/dry brain weights when more recently developed methods such as determining the T2 weight or analysis of magnetic resonance imaging or diffusion imaging might provide more appropriate information. In addition, we concentrated our analysis on the regions with the highest hepcidin expression analysis of different areas with different levels of expression which would provide some important details on the downstream target proteins. The downstream target protein levels will need to be investigated in the future.

## Conclusions

A rat model of SAH provided evidence that hepcidin was involved in the development of EBI. Hepcidin levels were increased by SAH and its downstream targets were decreased. EBI and apoptosis in the cerebral cortex were increased further by injection of hepcidin, but decreased by hepcidin-targeting siRNA. The present study on hepcidin and its inhibition provides a new strategy to treat SAH.

**Acknowledgments** This study was supported by the National Natural Science Foundation of China, National Clinical key specialty construction projects of China and funded project of Chongqing Science and Technology Commission.

## Compliance with ethical standards

**Conflict of interest** The authors declare that they have no conflict of interest.

**Ethical approval** All applicable international, national, and/or institutional guidelines for the care and use of animals were followed. The animal experimental ethics committee of Chongqing Medical University approved the experimental protocol.

## References

- Cahill J, Zhang JH (2009) Subarachnoid hemorrhage: is it time for a new direction? *Stroke* 40(3 Suppl):S86–S87. doi:10.1161/strokeaha.108.533315
- Ostrowski RP, Colohan AR, Zhang JH (2006) Molecular mechanisms of early brain injury after subarachnoid hemorrhage. *Neurol Res* 28(4):399–414. doi:10.1179/016164106x115008

3. Matz PG, Fujimura M, Chan PH (2000) Subarachnoid hemolysate produces DNA fragmentation in a pattern similar to apoptosis in mouse brain. *Brain Res* 858(2):312–319
4. He Z, Ostrowski RP, Sun X, Ma Q, Huang B, Zhan Y, Zhang JH (2012) CHOP silencing reduces acute brain injury in the rat model of subarachnoid hemorrhage. *Stroke* 43(2):484–490. doi:10.1161/strokeaha.111.626432
5. Park CH, Valore EV, Waring AJ, Ganz T (2001) Hepcidin, a urinary antimicrobial peptide synthesized in the liver. *J Biol Chem* 276(11):7806–7810. doi:10.1074/jbc.M008922200
6. Oliveira SJ, de Sousa M, Pinto JP (2011) ER stress and iron homeostasis: a new frontier for the UPR. *Biochem Res Int* 2011:896474. doi:10.1155/2011/896474
7. Nemeth E, Tuttle MS, Powelson J, Vaughn MB, Donovan A, Ward DM, Ganz T, Kaplan J (2004) Hepcidin regulates cellular iron efflux by binding to ferroportin and inducing its internalization. *Science* 306(5704):2090–2093. doi:10.1126/science.1104742
8. Li L, Holscher C, Chen BB, Zhang ZF, Liu YZ (2011) Hepcidin treatment modulates the expression of divalent metal transporter-1, ceruloplasmin, and ferroportin-1 in the rat cerebral cortex and hippocampus. *Biol Trace Elem Res* 143(3):1581–1593. doi:10.1007/s12011-011-8967-3
9. Pigeon C, Ilyin G, Courselaud B, Leroyer P, Turlin B, Brissot P, Loreal O (2001) A new mouse liver-specific gene, encoding a protein homologous to human antimicrobial peptide hepcidin, is overexpressed during iron overload. *J Biol Chem* 276(11):7811–7819. doi:10.1074/jbc.M008923200
10. Frazer DM, Anderson GJ (2003) The orchestration of body iron intake: how and where do enterocytes receive their cues? *Blood Cells Mol Dis* 30(3):288–297
11. Qian ZM, Wang Q (1998) Expression of iron transport proteins and excessive iron accumulation in the brain in neurodegenerative disorders. *Brain Res Brain Res Rev* 27(3):257–267
12. Klomp LW, Farhangrazi ZS, Dugan LL, Gitlin JD (1996) Ceruloplasmin gene expression in the murine central nervous system. *J Clin Invest* 98(1):207–215. doi:10.1172/jci118768
13. Wang Z, Meng CJ, Shen XM et al (2012) Potential contribution of hypoxia-inducible factor-1 $\alpha$ , aquaporin-4, and matrix metalloproteinase-9 to blood-brain barrier disruption and brain edema after experimental subarachnoid hemorrhage. *J Mol Neurosci* 48(1):273–280. doi:10.1007/s12031-012-9769-6
14. Chen Z, Gao C, Hua Y, Keep RF, Muraszko K, Xi G (2011) Role of iron in brain injury after intraventricular hemorrhage. *Stroke* 42(2):465–470. doi:10.1161/strokeaha.110.602755
15. Hockel K, Trabold R, Scholler K, Torok E, Plesnila N (2012) Impact of anesthesia on pathophysiology and mortality following subarachnoid hemorrhage in rats. *Exp Transl Stroke Med* 4(1):5. doi:10.1186/2040-7378-4-5
16. Tsubokawa T, Solaroglu I, Yatsushige H, Cahill J, Yata K, Zhang JH (2006) Cathepsin and calpain inhibitor E64d attenuates matrix metalloproteinase-9 activity after focal cerebral ischemia in rats. *Stroke* 37(7):1888–1894. doi:10.1161/01.str.0000227259.15506.24
17. Desland FA, Afzal A, Warraich Z, Mocco J (2014) Manual versus automated rodent behavioral assessment: comparing efficacy and ease of bederson and garcia neurological deficit scores to an open field video-tracking system. *J Cent Nerv Syst Dis* 6:7–14. doi:10.4137/JCNSD.S13194
18. Wang SM, Fu LJ, Duan XL, Crooks DR, Yu P, Qian ZM, Di XJ, Li J, Rouault TA, Chang YZ (2010) Role of hepcidin in murine brain iron metabolism. *Cell Mol Life Sci* 67(1):123–133. doi:10.1007/s00018-009-0167-3
19. Horvath LL, Pluta RM, Boock RJ, Oldfield EH (1998) Role of ferrous iron chelator 2,2'-dipyridyl in preventing delayed vasospasm in a primate model of subarachnoid hemorrhage. *J Neurosurg* 88(2):298–303. doi:10.3171/jns.1998.88.2.0298
20. Chi SI, Wang CK, Chen JJ, Chau LY, Lin TN (2000) Differential regulation of H- and L-ferritin messenger RNA subunits, ferritin protein and iron following focal cerebral ischemia-reperfusion. *Neuroscience* 100(3):475–484
21. Gitlin JD (1998) Aceruloplasminemia. *Pediatr Res* 44(3):271–276. doi:10.1203/00006450-199809000-00001
22. Jomova K, Vondrakova D, Lawson M, Valko M (2010) Metals, oxidative stress and neurodegenerative disorders. *Mol Cell Biochem* 345(1–2):91–104. doi:10.1007/s11010-010-0563-x
23. Ong WY, Halliwell B (2004) Iron, atherosclerosis, and neurodegeneration: a key role for cholesterol in promoting iron-dependent oxidative damage? *Ann N Y Acad Sci* 1012:51–64
24. Ghribi O, Golovko MY, Larsen B, Schrag M, Murphy EJ (2006) Deposition of iron and beta-amyloid plaques is associated with cortical cellular damage in rabbits fed with long-term cholesterol-enriched diets. *J Neurochem* 99(2):438–449. doi:10.1111/j.1471-4159.2006.04079.x
25. Chan PH (2001) Reactive oxygen radicals in signaling and damage in the ischemic brain. *J Cereb Blood Flow Metab* 21(1):2–14. doi:10.1097/00004647-200101000-00002
26. Yeo JE, Kang SK (2007) Selenium effectively inhibits ROS-mediated apoptotic neural precursor cell death in vitro and in vivo in traumatic brain injury. *Biochim Biophys Acta* 1772(11–12):1199–1210. doi:10.1016/j.bbadis.2007.09.004
27. Nguyen TT, Cho SO, Ban JY, Kim JY, Ju HS, Koh SB, Song KS, Seong YH (2008) Neuroprotective effect of *Sanguisorba radix* against oxidative stress-induced brain damage: in vitro and in vivo. *Biol Pharm Bull* 31(11):2028–2035
28. Matz PG, Fujimura M, Lewen A, Morita-Fujimura Y, Chan PH (2001) Increased cytochrome c-mediated DNA fragmentation and cell death in manganese-superoxide dismutase-deficient mice after exposure to subarachnoid hemolysate. *Stroke* 32(2):506–515
29. He Z, Ostrowski RP, Sun X, Ma Q, Tang J, Zhang JH (2012) Targeting C/EBP homologous protein with siRNA attenuates cerebral vasospasm after experimental subarachnoid hemorrhage. *Exp Neurol* 238(2):218–224. doi:10.1016/j.expneurol.2012.08.025